Quantum entanglement with acousto-optic modulators: Two-photon beats and Bell experiments with moving beam splitters

André Stefanov,[1,*] Hugo Zbinden,[1] Nicolas Gisin,[1] and Antoine Suarez[2]
[1]*Group of Applied Physics, University of Geneva, 1211 Geneva 4, Switzerland*
[2]*Center for Quantum Philosophy, P.O. Box 304, 8044 Zurich, Switzerland*
(Received 2 October 2002; published 29 April 2003)

We present an experiment testing quantum correlations with frequency shifted photons. We test Bell inequality with two-photon interferometry where we replace the beam splitters with acousto-optic modulators, which are equivalent to moving beam splitters. We measure the two-photon beats induced by the frequency shifts, and we propose a cryptographic scheme in relation. Finally, setting the experiment in a relativistic configuration, we demonstrate that the quantum correlations are not only independent of the distance but also of the time ordering between the two single-photon measurements.

DOI: 10.1103/PhysRevA.67.042115 PACS number(s): 03.65.Ta, 03.65.Ud, 03.30.+p, 03.67.Hk

I. INTRODUCTION

Entanglement is a basic resource for quantum information processing as well as for fundamental tests of quantum mechanics. Several types of entanglement between photons have already been demonstrated: polarization entanglement [1], energy-time entanglement [2–4], and time-bin entanglement [5,6], see Ref. [7] for a review. In this paper, we present a setup based on energy-time entanglement, where we add a frequency shift in one arm of each interferometer. Experimentally, the frequency shift is induced by using acousto-optic modulators (AOMs) in the interferometers instead of standard beam splitters.

Section II of this paper is devoted to the effects of a frequency shift on the time-dependent coincidence rate in a Franson-type Bell experiment. This effect is equivalent, for two-photon interferences, to the phenomenon of beats for single-photon interferences. As the time needed to record interference fringes cannot be arbitrarily small, the measured visibility is reduced in the presence of beats. When this measurement time is only limited by energy resolution, there is a simple relation between the visibility and the which-path information. Experimentally, we are far from acceding to very short measurement times, therefore we propose an indirect method to show the beats.

Section III presents the experimental setup in detail and the techniques used to overcome the difficulties due to the frequency shifts. We have measured high visibility interference fringes when the beats are canceled, and we have also measured the beats frequency when it is not zero.

Since an AOM is equivalent to a moving beam splitter, our setup can be used to perform experiments with apparatuses in two different relevant frames [8]. In the conventional experiments with all apparatuses at rest, there is only one relevant inertial frame, i.e., one inertial frame of the massive pieces of the apparatus (the laboratory frame) and, therefore, only one possible time ordering: one of the photons is always measured before the other (*before-after* situation). Using two relevant frames it is possible to create a *before-before* time ordering, in which each measuring device in its own inertial frame analyzes the corresponding photon before the other, and an *after-after* time ordering, in which each measuring device in its own inertial frame analyzes the corresponding photon after the other [9,10]. Quantum mechanics predicts correlations independently of the time ordering, between the two single-photon measurements. By contrast, multisimultaneity [11], a recently proposed alternative theory, casts nonlocality into a time-ordered scheme and predicts disappearance of nonlocal correlations with before-before timing. Therefore, experiments with AOMs allow us to test a most important feature of quantum entanglement as it is the independence of the time ordering. This is the subject of Sec. IV.

II. TWO-PHOTON BEATS

When two monochromatic waves of frequencies ω_1 and ω_2 are combined, the resulting wave exhibits two frequencies, one at $\omega_0=(\omega_1+\omega_2)/2$ and the other at $\delta\omega=(\omega_1-\omega_2)/2$. This is the well-known phenomenon of beats. An application in the optical domain for classical light field is heterodyne detection [12].

Beats can be seen as first-order interferences in the time domain. For second-order interferences, the same equivalence can be found. Consider the Franson-type configuration of Fig. 1; a source S emits energy-time entangled pairs of photons. Each photon is sent to an unbalanced interferometer. When both photons arrive in coincidence on the detectors, it is impossible to distinguish between both photons passing by the short arms (ss) or both passing by the long ones (ll) because the photon emission time is undetermined. Hence interference fringes appear when the phases ϕ_i are changed. In our experiment, we consider not only phase changes in each interferometer but also changes of the photon frequencies. When both frequency shifts do not sum to 0 we will show that the coincidence rate between two detectors changes periodically in time. This is equivalent, for two-photon interferences, to the phenomenon of beats in one-photon interferences; therefore, we call it two-photon beats.

Following closely Franson's calculation [2], the wave function at detector D_i, $i\in\{a,b\}$, located at r_i, is given by

*Email address: Andre.Stefanov@physics.unige.ch

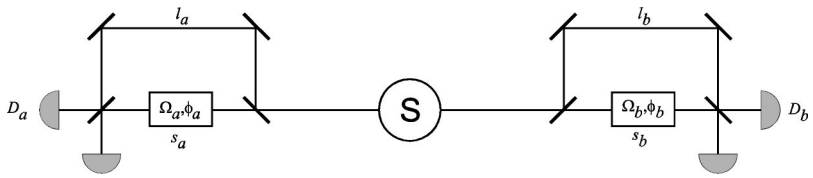

FIG. 1. Franson-type Bell experiment with frequency shift. l_i and s_i are the lengths of the long and short arms of interferometer i, Ω_i and ϕ_i are the frequency shift and phase shift in the short arm of interferometer i.

$$\Psi(r_i,t)=\frac{1}{2}\Psi_0(r_i,t)+\frac{1}{2}e^{i\phi_i}\Psi_0^{\Omega_i}(r_i,t-\Delta t_i), \qquad (1)$$

where ϕ_i is the phase of interferometer i, $c\Delta t_i=\Delta l_i=l_i-s_i$ is the path difference between both arms of the interferometer and Ω_i is the frequency shift in the short arm of interferometer i. The difference with Franson's original calculation is that we consider an arbitrary frequency shift Ω_i in one arm of the interferometers. We can expand the wave functions in the field operators c_k,

$$\Psi_0(r_i,t)=\sum_k c_k e^{i(kr_i-\omega_i t)},$$

$$\Psi_0^{\Omega_i}(r_i,t)=\sum_k c_k e^{i(kr_i-(\omega_i+\Omega_i)t)}, \qquad (2)$$

where ω_i is the frequency of the photon in interferometer i. The coincidence rate between two detectors is then given by

$$R=\langle 0|\Psi^+(r_a,t)\Psi^+(r_b,t)\Psi(r_b,t)\Psi(r_a,t)|0\rangle. \qquad (3)$$

Using Eqs. (1) and (2) in Eq. (3) we find

$$R\sim\frac{1+\cos(\omega_0\Delta t+\Omega^0\Delta t+\phi_1+\phi_2-\Omega^0 t)}{2}, \qquad (4)$$

where $\Omega^0=\Omega_a+\Omega_b$. This corresponds to Franson's result, when $\Omega^0=0$, otherwise the coincidence probability is generally not constant in time.

When the entangled photons are created by down-conversion [13], we have to take into account the finite bandwidth of the pump laser and of the photons. We find, assuming Gaussian spectral distributions, that the coincidence probability is given by

$$R=\frac{1+\chi\cos(\omega_0\Delta t+\Omega^0\Delta t+\phi_1+\phi_2-\Omega^0 t)}{2}, \qquad (5)$$

with

$$\chi=f\left(\frac{\Delta l_b}{c},\delta\omega_0\right)f\left(\frac{\Delta l_a-\Delta l_b}{c},\Delta\right), \qquad (6)$$

where $f(x,y)=\exp(-\frac{1}{2}x^2y^2)$, ω_0 is the central frequency of the pump laser, $\delta\omega_0$ is the pump bandwidth, and Δ is the photon bandwidth. Hence the visibility of the interference fringes is reduced by a factor χ. In absence of beats ($\Omega^0=0$), χ is the maximal visibility that can be measured. Equation (6) contains all the usual conditions to see high visibility interference fringes; the coherence length of the pump laser has to be greater than the path difference in one interferometer, and the photon coherence length has to be greater than the difference $\Delta l_a-\Delta l_b$.

An application of entangled photons, apart from fundamental tests of quantum mechanics, is quantum cryptography. Setups based on polarization, energy-time or time-bin entanglement have been proposed and realized, for a review see Ref. [14]. One the other hand, only one-photon schemes with frequency shifted photons have been proposed [15,16]. In Appendix A we propose two different schemes with frequency shifted entangled photons, which can be used to implement quantum cryptography, although they are not actually of practical interest, due to technological limitations.

A. Frequency shift as quantum eraser

If the beat frequency is not zero, the coincidence probability changes in time, decreasing the visibility of the interference fringes. According to the Feynman ''principle'' [17], the disappearance of the interference fringes would imply accessibility, in principle, of information about which path the photons took [18]. The frequency shift can be used to mark the path, only if we have enough coincidence events such that the time needed to experimentally estimate the coincidence probability is smaller than the intrinsic uncertainty Δt on the time measurement given by saturating the energy-time uncertainty relation $\Delta E\Delta t=\hbar$. Otherwise, information about the path is lost due to imperfect experimental devices.

We can quantify this information and the corresponding loss of visibility. Contrary to Ref. [19] where the degree of freedom used to mark the photon (i.e., polarization) is different from the one where interferences are observed (spatial mode), we use the frequency to mark the paths. This will affect the interferences by creating beats as we have shown before. However, due to the energy-time uncertainty relation there is still a relation between interferences' visibility and the which-path information.

If the time needed to measure the coincidence probability is arbitrarily small: $\Delta t=0$, the coincidence probability will be given by $[1+\cos(\Phi-\Omega^0 t)]/2$, according to Eq. (5) where we assume $\chi=1$ and $\Phi=\omega\Delta t+\Omega^0\Delta t+\phi_1+\phi_2$. For a finite time resolution we have to integrate this expression over a time distribution with a width Δt, for example, we consider a Gaussian distribution

$$p=\int_{-\infty}^{\infty}\frac{1+\chi\cos(\Phi-\Omega^0 t)}{2}\frac{1}{\sqrt{2\pi}\Delta t}\exp\left(-\frac{1}{2}\frac{t^2}{\Delta t^2}\right)dt$$

$$=\frac{1}{2}+\frac{1}{2}\cos(\Phi)\exp\left(-\frac{1}{2}(\Omega^0)^2\Delta t^2\right). \qquad (7)$$

The corresponding visibility is

$$V(\Delta t)=\frac{p_{max}-p_{min}}{p_{max}+p_{min}}=\exp\left(-\frac{1}{2}(\Omega^0)^2\Delta t^2\right). \quad (8)$$

The which-path information is given by measuring the total energy of the photons ω. This is done with a resolution $\Delta\omega$ related to the time resolution by the energy-time uncertainty relation $\Delta\omega\Delta t\geqslant 2\pi$. We predict that the photons would be detected in the ll arm if we measure $\omega<\omega_0+\Omega^0/2$, and in the ss arm otherwise. The which-path information K is given by $K=2q-1$ [20] where q is the probability of a correct prediction on the path. With our strategy we have

$$q=p(ll|\omega<\omega_0+\Omega^0/2)$$
$$=1-\frac{1}{\sqrt{2\pi}\Delta\omega}\int_{\omega_0+\Omega^0/2}^{\infty}\exp\left(-\frac{1}{2}\frac{(\omega-\omega_0)^2}{\Delta\omega^2}\right)d\omega. \quad (9)$$

Hence the information is given by

$$K=2\,\mathrm{erf}\left(\frac{\Omega^0\Delta t}{4\sqrt{2}\pi}\right)-1 \quad (10)$$

with $\mathrm{erf}(x)$ being the error function. The extreme cases are either a perfect distinction between ss and ll events, which requires that $\Delta E\ll\hbar\Omega^0$, but this implies a measurement time $\Delta t\gg 1/\Omega^0$, averaging to zero the interferences; or, on the contrary, if the measuring time is short enough to measure interference, then the energy resolution is too poor to distinguish the paths. For the intermediate case we have the known relation [20] $V^2+K^2\leqslant 1$. The equality is not reached because the prediction strategy is not optimal.

Let us emphasize that the preceding description does not rely on quantum mechanics but more generally on wave theory. The quantum nature appears when we assume that photons are quanta of light, and in the fact that the photon pairs we consider cannot be described by classical local physics.

B. Measurements of two-photon beats

In our experiment, when the radio-frequency drivers are not synchronized, the minimum value that can be set for $2\pi\Omega^0$ is 31.5 kHz. This is too large to directly see the beats by recording the coincidence rate vs time. A first possible method is to record the time of each coincidence event and reconstruct the beats from those data. This requires a clock precise enough over a long time. However, this requires also that the coherence of the beats signal is much longer than the acquisition time, so that the phases of the interferometers have to be kept stable during that time. We also need to know precisely the frequency Ω^0, otherwise the analysis of the data will be much more complicated, although not impossible.

Instead of recording all the absolute times of arrival and reconstruct the beats, we could only measure the time difference between two successive coincidence counts and then measure the distribution of those times.

The probability density $P(\Delta t)$ of having two coincidences separated by a time Δt can be computed in the following way. Since the detection process is independent of time, the conditional probability of having a coincidence at time t and another one at time $t+\Delta t$, knowing that a photon pair reaches the detectors at time t and another one at time $t+\Delta t$, is only dependent on the beats signal,

$$p(t,t+\Delta t|\gamma_t,\gamma_{t+\Delta t})$$
$$=C\frac{1+V\cos(\Omega^0 t)}{2}\frac{1+V\cos[\Omega^0(t+\Delta t)]}{2}, \quad (11)$$

where V is the visibility and C is a normalization constant. Without loss of generality, we can assume that the efficiency of the detectors is 1 and the detectors do not have a dead time. This is justified because, the real dead time of the detectors is much smaller than the time interval between two detections and also much smaller than the beats period.

We do not access the time t but we only measure Δt. Therefore the probability of having two coincidences, knowing only that the second photon comes at Δt after the first, is given by

$$p(\Delta t|\gamma_{\Delta t})=\frac{\Omega^0}{2\pi}\int_0^{2\pi/\Omega^0}p(t,t+\Delta t|\gamma_t,\gamma_{t+\Delta t})dt. \quad (12)$$

The integration gives

$$p(\Delta t|\gamma_{\Delta t})=C\frac{1}{4}\left[1+\frac{V^2}{2}\cos(\Omega^0\Delta t)\right]. \quad (13)$$

Finally, the probability density of having two coincidences separated by a time Δt is obtained using the fact that the emission and detection are two Poissonian processes independent of the beats. Therefore, the probability $dp_{emission}(\Delta t)$ of having two emissions separated by a time Δt is

$$dp_{emission}(\gamma_{\Delta t})=\frac{1}{\tau}\exp(-\Delta t/\tau)d(\Delta t). \quad (14)$$

Hence, the probability density $P(\Delta t)$ of having two coincidence events separated by a time Δt is given by

$$dp(\Delta t)=p(\Delta t|\gamma_{\Delta t})dp_{emission}(\gamma_{\Delta t})=CP(\Delta t)d(\Delta t) \quad (15)$$

with $P(\Delta t)=\frac{1}{4}[1+(V^2/2)\cos(\Omega^0\Delta t)](1/\tau)\exp(-\Delta t/\tau)$. We normalize this expression such that

$$1=\int_0^{\infty}P(\Delta t)d(\Delta t)=C\frac{1}{8}\left(2+\frac{V^2}{1+(\Omega^0)^2\tau^2}\right). \quad (16)$$

The final normalized expression is then

$$P(\Delta t)=\frac{\left[1+\frac{V^2}{2}\cos(\Omega^0\Delta t)\right]\exp(-\Delta t/\tau)}{\tau\left(1+\frac{V^2}{2}\frac{1}{1+(\Omega^0)^2\tau^2}\right)}. \quad (17)$$

Experimentally, we integrate $P(\Delta t)$ over a time bin t_b so that the measured probability is

$$p(\Delta t)=\int_{\Delta t}^{\Delta t+t_b/2}P_N(t')dt'. \quad (18)$$

The total count N_c in m seconds in each time bin is

$$N_c(\Delta t)=\frac{m}{\tau}p(\Delta t). \quad (19)$$

The advantage of this method to see two-photon beats is that the interferometer only needs to be stable during the time between two successive coincidences. In Sec. III F, we present the results of the beats frequency using this method.

III. EXPERIMENTAL SETUP

A. Principle

The setup we use to test entanglement of the photon pairs with frequency shift is based on previous Franson-type experiments [21]. The main conceptual difference is the frequency shifts in one arm of the interferometers.

B. Source

The photon pairs are created by parametrical down-conversion in a recently developed high efficient source. It is based on a waveguide integrated on a periodically poled lithium niobate (PPLN) substrate [22]. Using a pump at 657 nm, it generates degenerated photons at 1314 nm. We chose this wavelength as it corresponds to a transparency window in optical fibers. Hence it is possible to use this setup for long-distance transmission. An RG1000 filter is placed after the waveguide to eliminate the pump light, and an additional interference filter is used to narrow the generated photon's bandwidth. The photon pairs are coupled into a 50/50 fiber-optics beam splitter that separates the twin photons.

Violation of Bell inequality has already been demonstrated with this source [23].

C. Acousto-optic modulator as a moving beam splitter

As for Franson-type experiments, we use Michelson interferometers as analyzers. We replaced in each interferometer the beam splitters by AOMs (Brimrose AMF-100, 1.3–2 mm). They have two effects. First they induce a frequency shift equal to the acoustic wave frequency as we will see, second they can be seen as moving beam splitters as required for a relativistic Bell experiment [11].

An AOM is made of a piece of glass, AMTIR 1 (amorphous material transmitting infrared radiation), in which an acoustic wave at frequency Ω (100 MHz in our experiment) is created by a piezoelectrical transducer [24]. As the refractive index in a material depends on the pressure, the acoustic wave will create a periodic change of the refractive index, equivalent to a diffraction grating (Fig. 2). If the acoustic wave is traveling rather than being stationary, it will be equivalent to a *moving* diffraction grating. This can be achieved if the AOM ends with a skew cut termination to dampen the wave. As for a standard grating, the reflection coefficient is maximal at Bragg angle θ_B given by

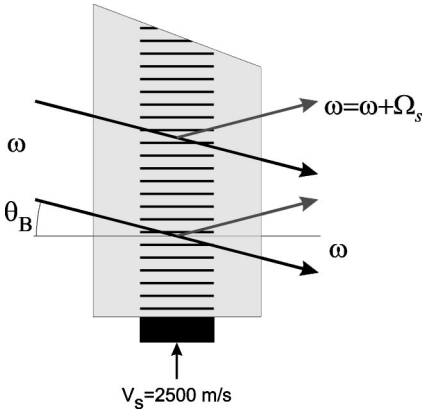

FIG. 2. Acousto-optic modulator, the Bragg grating created by a sound wave of frequency Ω_s reflects part of the incoming light, whose frequency is ω.

$$2\lambda_s\sin\theta_B=\lambda/n, \quad (20)$$

where λ_s is the sound wavelength, λ is the light wavelength in vacuum, and n is the refractive index of the material. The reflection coefficient is, for small angles θ_B [25],

$$R=\frac{\pi^2}{2\lambda^2}\left(\frac{L}{\sin\theta_B}\right)^2\mathcal{M}I, \quad (21)$$

where I is the acoustic power, $L/\sin\theta_B$ is the penetration of light through the acoustic wave, and $\mathcal{M}$ is a material parameter. The acoustic power can be set such that the beam splitting ratio is 50/50.

The reflected wave undergoes a frequency shift of $+\Omega$ if it hits the acoustic wave in the same direction as Fig. 2, in the opposite case the frequency shift is $-\Omega$.

The reflection on a moving mirror produces a frequency change of the light [11], due to the Doppler effect, given by

$$\Delta\nu=\frac{2nv\sin\theta}{c}\nu, \quad (22)$$

where v is the mirror velocity and θ is the angle between the incident light and the plane of reflection. Within an AOM, the reflected light is also frequency shifted and the frequency shift is equal to the acoustic wave frequency:

$$\Delta\nu=\Omega. \quad (23)$$

Using $\lambda_s\Omega=v_s$, $\theta=\theta_b$, and Eqs. (20) and (23) we find that the frequency shift induced by the AOM is the same as the one induced by a mechanical grating traveling at speed v_s. The velocity of sound in the AMTIR 1 can be computed

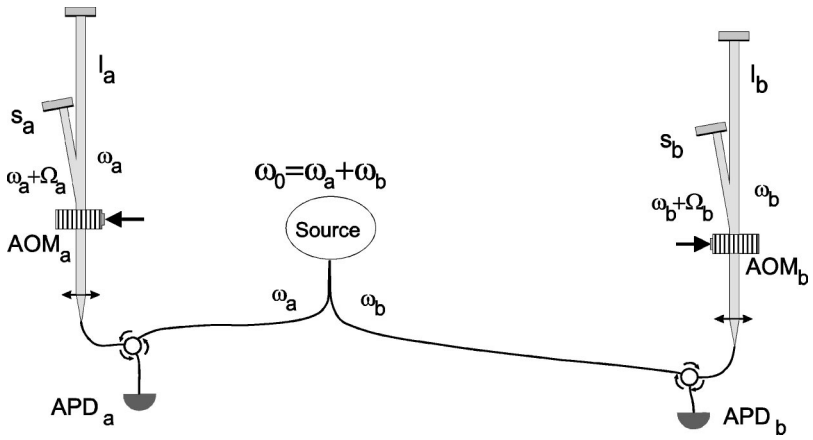

FIG. 3. Schematic of the experiment, the AOMs are oriented such that both sound waves travel in the opposite direction and such that the frequency shifts of the reflected wave are of opposite signs. The total energy of both photons after the source is ω_0. When both photons pass through the long arms, the total energy is not changed, but when they pass through the short arms the total energy becomes $\omega_a+\omega_b+\Omega_a+\Omega_b$. It is required that $\Omega_a+\Omega_b=0$ to avoid that beats hide the correlations.

from the mechanical parameters of the material. The velocity for primary sound waves [26] is given by

$$v_s=\sqrt{\frac{\lambda+2\mu}{\rho}}, \tag{24}$$

where $\mu=E/[2(1+\nu)]$ and $\lambda=E\nu/[(1+\nu)(1-2\nu)]$, E is the Young's modulus and ν is the Poisson ratio. For AMTIR 1 we have [27] $E=21.9\times10^9$ Pa, $\nu=0.266$, and $\rho=4.41\times10^3$ kg/m^3, hence $v_s=2480$ m/s. This corresponds to the manufacturer value of $v_s=2500$ m/s.

The phase of the reflected wave is also shifted by a value φ which is the phase of the acoustic wave at the time when the light is reflected.

D. Two-photon interferometry with frequency shifts

We have built two bulk Michelson interferometers using AOMs instead of beam splitters. The light is coupled out of the fiber using an angle physical contact connector to avoid back reflection at the fiber's end. Because of the small deviation angle $2\theta_b$ (about 5°), we collect only the light coming back into the input port by using a fiber-optical circulator (Fig. 3). Due to imperfect overlap of the modes, the transmission through each interferometer is about 45%, with monochromatic light. The transmission through the reflected arm is reduced for large bandwidth photons, because the deviation angle depends on the light's wavelength. Hence, an AOM will act as a bandpass filter for the reflected beam with a measured bandwidth of about 30 nm. To minimize this effect, which could reduce the fringe's visibility, we have to ensure that the bandwidth of the photons is smaller by placing after the source a spectral filter (11 nm bandwidth).

The condition to observe interferences is given by Eq. (6). It is the usual condition for two-photon correlations that the path differences Δl_i between the short and the long arm of the interferometers have to be equal within the coherence length of the photons. Without frequency shifts ($\Omega_a=\Omega_b=0$) the equalization of the paths of both interferometers can be done by putting them in series [21] (Fig. 4) and looking for the interferences between the $s_a l_b$ and $l_a s_b$ paths. Using a low coherence light, interferences appear only when s_a+l_b is equal to l_a+s_b within the coherence length of the light. This implies that $\Delta l_a=\Delta l_b$ (in our interferometers $\Delta l_i/c\simeq1.5$ ns). Unfortunately, this method cannot directly work when there is a frequency shift. Indeed when we put our interferometers in series, with the AOMs oriented as for the two-photon experiment, the frequency shifts do not cancel anymore but beats appear between the $s_a l_b$ and $l_a s_b$ paths at the frequency of $\Omega_a-\Omega_b=400$ MHz. In order to observe those beats, we use a fast *p*-intrinsic-*n* (PIN) detector (2 GHz bandwidth) connected to an electrical spectrum analyzer. As such a detector is not very sensitive, so we use a very bright light-emitting diode (LED) source (Opto Speed SA SLED 1300-D10A). With this setup, it is easy to scan the long path of one of the interferometers until we see classical beats.

Once the path-length differences are equalized we can look for the two-photon interference with the setup of Fig. 3. Therefore, the frequency shifts have to cancel each other such that $\Omega^0=0$ [Eq. (4)]. We orient the AOM as described such that the frequency shifts are of opposite signs (Fig. 3). Hence we have $\Omega_a=200$ MHz (because we pass two times through each AOM) and $\Omega_b=-200$ MHz.

Experimentally, we can only specify an upper bound on $|\Omega^0|$. The requirement is given by the fact that we have to integrate over times much larger than $1/\Omega^0$ to estimate the coincidence probability with small statistical error (typically 10–20 s). Therefore, even if the temporal resolution of the detectors would have been good enough to see interference fringes in principle [Eq. (8)], the integration cancels them. Hence we can only see interference fringes if $\Omega^0<10^{-2}$.

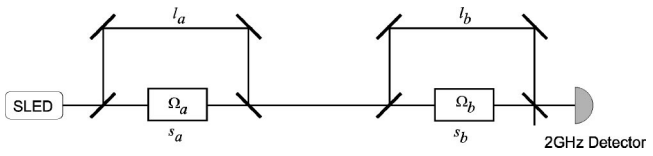

FIG. 4. Principle of alignment of the interferometer path difference. Experimentally, Michelson interferometers were used.

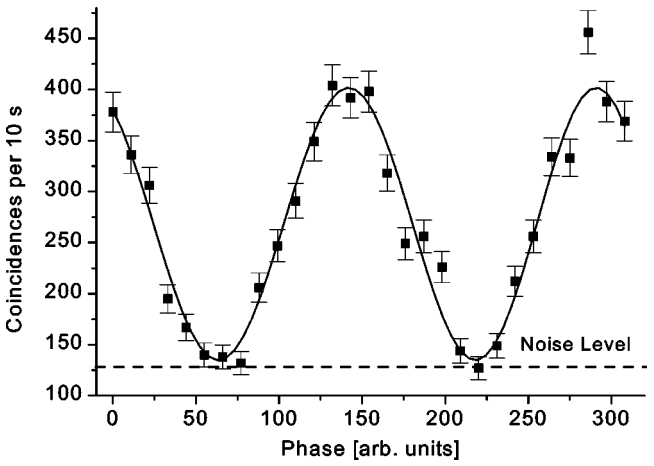

FIG. 5. Interference fringes. The dashed line indicates the noise level, which is the rate of accidental coincidences. The visibility after subtraction of the noise is $(97\pm5)\%$.

Otherwise we have to use indirect means of observing the beats, as described in the following section.

Finally, one should note that if the frequency shift Ω is greater than the photon bandwidth $\delta\omega_0$,

$$\Omega \gg \delta\omega_0, \tag{25}$$

it will be possible to distinguish the path by measuring only the energy of one photon. In that case the correlations disappear because the phase shift on the reflected wave will not be well defined as the mirror is moving. More precisely this phase change due to the change of the mirror position during the coherence time $\delta\tau$ of the photon is given by

$$\Phi = \frac{\delta\tau v_s}{\lambda_s} = \frac{\Omega}{\delta\omega_0}. \tag{26}$$

Interference fringes can be seen only if $\Phi \ll 1$, which is in contradiction with Eq. (25).

E. Synchronization

Each AOM is driven by a radio-frequency driver (Brimrose FFF-100-B2-V0.8-E) which generates a 100 MHz. As we have seen we need to synchronize the radio-frequency drivers with a frequency difference smaller than 10^{-2} Hz. This is done by using the fact that the 100 MHz frequency is generated in each driver by multiplying a 1-MHz signal from an oscillator with a phase-locked loop. The synchronization is achieved by using the same oscillator for both drivers. In practice we send the signal from one of the driver's oscillator to the other driver through a coaxial cable. The ratio of the frequencies, measured with a frequency meter, is 1 ± 10^{-11}, so that $\Omega^0 < 10^{-2}$ Hz. Another point to look at is the shape of the electrical spectrum on both sides. We verified with a spectrum analyzer that both spectrum widths are smaller than the resolution of the analyzer (100 Hz).

Once the synchronization is correctly done we observe interference fringes with high visibility (Fig. 5). The visibility after subtracting the accidental coincidences is about 97%. The visibility without subtracting the noise is about 45%.

We have verified that the visibility is reduced when the electrical spectra of the drivers are slightly different. The frequency of one of the drivers can be changed by steps of 15 625 Hz. Due to beats, no interference fringes can be observed when the drivers are set at different frequencies.

The phase difference ϕ_{AOM} between the two synchronized acoustic waves induces the same phase change in the two-photon interference fringes. ϕ_{AOM} depends on the length l of the synchronization cable,

$$\phi_{AOM} = \alpha l + \phi_0, \tag{27}$$

where

$$\alpha = \frac{2\pi}{\lambda_{synch}} \frac{\nu_{AOM}}{\nu_{synch}} \tag{28}$$

with λ_{synch} and ν_{synch} being the wavelength and frequency of the 1-MHz synchronization signal. Hence we have

$$\alpha = \frac{2\pi\nu_{AOM}}{v_{synch}} \tag{29}$$

with v_{synch} the speed of the synchronization signal. We can measure α by changing the length of the synchronization cable and measuring the induced phase shift on the interference fringes. We clearly observe a frequency shift when we add or remove 0.53 m or 1.03 m of cable (Fig. 6). The mean phase shift per meter α of cable added on five measurements is 6.97 ± 0.09 rad/m. Hence, with $\nu_{AOM}=2\times10^8$ Hz, $v_{synch}=0.60c\pm0.01c$. This is compatible with the speed of signal propagation in coaxial cables.

F. Experimental evidence of two-photon beats

We use the procedure described previously to experimentally show two-photon beats, when the difference of frequencies $\Omega^0/2\pi$ is 31 250 Hz. We have measured the time difference between successive coincidences and we plot the histogram of those measurements. The time bins of the histogram are of 4×10^{-6} s and we plot it for times between 0 s and 0.1 s. Fig. 7 shows the exponential decrease, as expected for random events. However, on closer inspection we see that the exponential decay is modulated by a cosine (Fig. 8). We fit an approximation of Eq. (19),

$$N_c(t) = \frac{m}{\tau}p(t) \cong \frac{m}{\tau}t_B \frac{\left[1+\frac{V^2}{2}\cos(\Omega t)\right]\exp(-t/\tau)}{\tau\left(1+\frac{V^2}{2}\frac{1}{1+\Omega^2\tau^2}\right)}, \tag{30}$$

because the width of the histogram time bins is small enough $(t_B \ll 1/\Omega)$.

The visibility given by the fit ($V=0.448$, $\Omega=196\,350$, $\tau=0.0163$, $\phi=1.86$, $m=13\,091$) is compatible with the direct measurements of visibility and the frequency that we

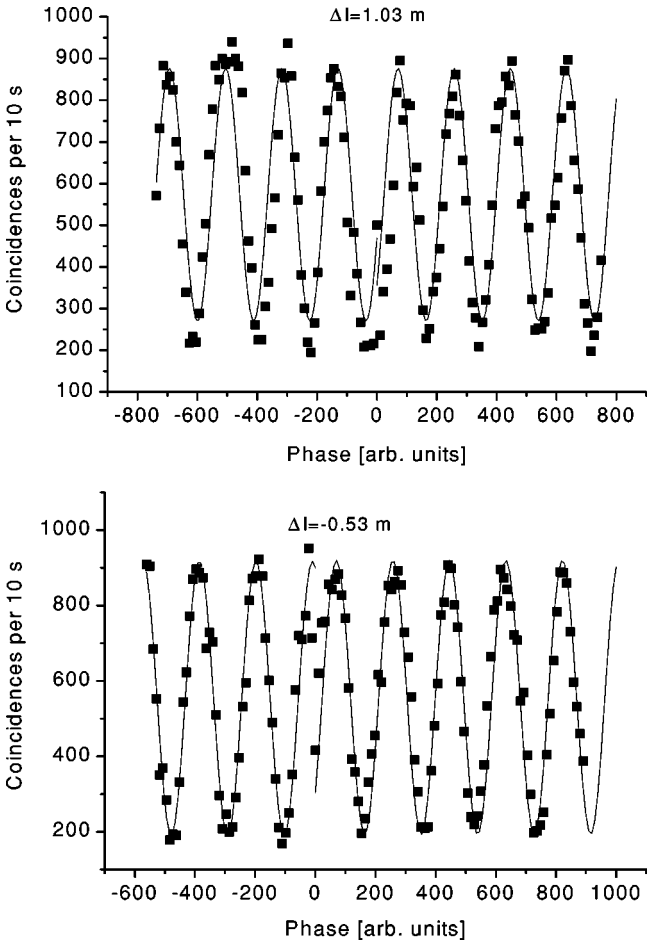

FIG. 6. Phase shift of the coincidence rate when the synchronization cable length is changed. Upper graph: 1.03 m is added, the phase shift given by the fit is $\Delta\phi_{AOM}=6.73\pm0.20$ rad. Lower graph: 0.53 m is subtracted, the phase shift given by the fit is $\Delta\phi_{AOM}=-3.61\pm0.07$ rad.

found is $\nu=31\,250.0\pm1.6$ Hz, as expected. Another measurement with a frequency shift of 62.5 kHz gives similar results.

IV. MULTISIMULTANEITY

A. Motivation

Classically, correlations between separated events can be explained by two different mechanisms: either both events have a common cause in the past, e.g., two separate TV apparatuses showing the same images because they are connected to the same channel; or one event has a direct influence on the other, e.g., dialing a number on my phone makes the phone of my colleague ring. In both cases there is a time-ordered causal relation.

Quantum correlations, on the other hand, are of very different nature. Quantum mechanics predicts correlated outcomes in spacelike separated regions for experiments using pairs of entangled particles. Many experiments have demonstrated such quantum correlations, under several conditions [4,28], in perfect concordance with the quantum-mechanical

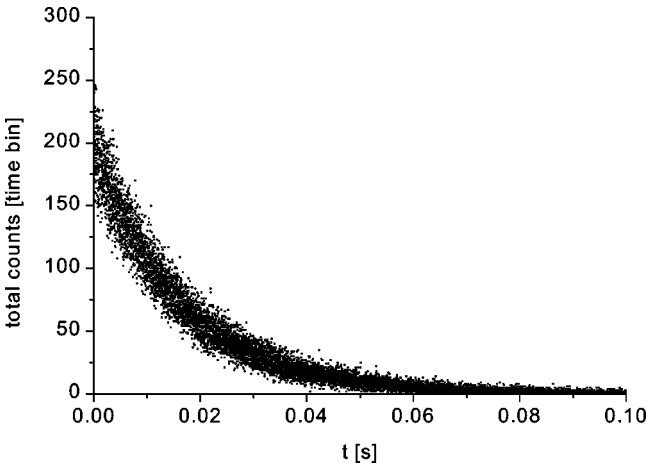

FIG. 7. Histogram of the time difference between successive coincidences (large scale). This graph shows an exponential decrease because the photon pair detection is a Poissonian process.

predictions. The existence of correlations shows that the outcomes of the two measurements are not independent. However, in that case, violation of Bell inequality rules out the common cause explanation [29].

To explain the correlations one could impose a possible influence of one outcome on the other. Since the correlated events lie in spacelike separated regions, such a direct influence would have to be superluminal. Moreover, this would define a preferred frame, because the time ordering between two spacelike separated events is not relativistically covariant.

One could imagine a unique preferred frame which is relevant for all the quantum measurements. The pilot-wave model of de Broglie and Bohm [30] assumes such a preferred frame. This model perfectly reproduces the results of quantum mechanics, and the assumed connections, though superluminal, cannot be used for faster than light communication [31]. Moreover, since quantum mechanics is independent of the timing, Bohm's preferred frame is experimentally indistinguishable. Another theory assuming a unique preferred frame has been proposed by Eberhard [32]. In this

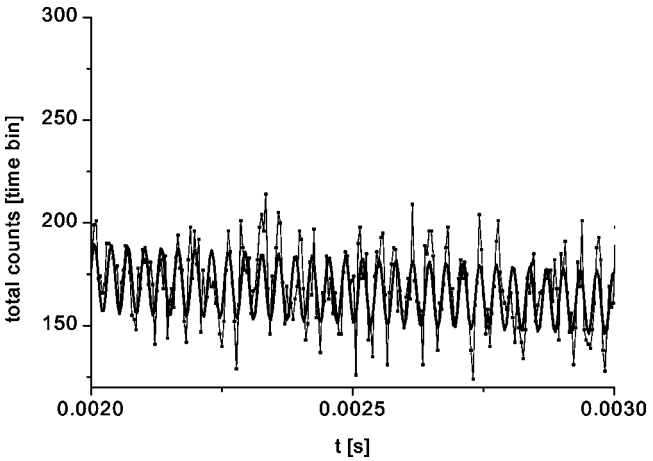

FIG. 8. Histogram of the time difference between successive coincidences (small scale).

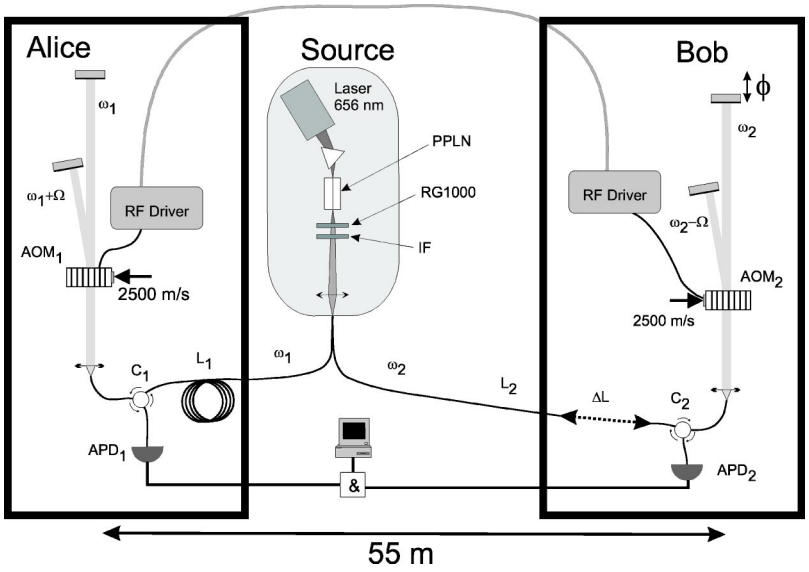

FIG. 9. Schematic of the experiment. The high efficiency photon pair source uses a PPLN waveguide pumped by a 656-nm laser. An RG1000 filter is used to block the pump laser and a 11-nm-large interference filter (IF) narrows the photon bandwidth. The two AOMs are 55 m apart and oriented such that the acoustic waves propagate in opposite directions. One output of the interferometers is collected back, thanks to optical circulators C_1 and C_2, and the detection signals are sent to a coincidence circuit. As the frequency shifts are compensated, the total energy when both photons take the short arms or the long ones is constant. Two-photon interference fringes are observed by scanning the phase ϕ.

model the connection between the events is not only superluminal but it propagates at a finite speed, and leads to faster than light communication. If, in the preferred frame, both choices occur in a short enough time interval, the correlations would disappear as the influences would not have the time to propagate. However, experimentally this theory cannot be refuted, because the speed of the influence can be arbitrarily large and is not specified by the theory.

A different natural possibility would be to assume that the relevant reference frame for each measurement is the inertial frame of the massive apparatus, and to define a time-ordered dependence by means of several preferred frames. This possibility has been developed within a theory called multisimultaneity [10]. More specifically, multisimultaneity assumes that the relevant frame is determined by the analyzer's inertial frame (e.g., a polarizer or a beam splitter in our case). Paraphrasing Bohr, one could say that the relevant frame, hence the relevant time ordering, depends on the very condition of the experiment [33].

In multisimultaneity, as in the pilot-wave model, each particle emerging from a beam splitter follows one (and only one) outgoing mode, hence particles are always localized, although the guiding wave (i.e., the usual quantum state ψ) follows all paths, in accordance with the usual Schrödinger equation. When all beam splitters are at relative rest, this model reduces to the pilot-wave model and has thus precisely the same predictions as quantum mechanics. However, when two beam splitters move apart, there are two relevant reference frames, each defining a time ordering, hence the name of multisimultaneity. In such a configuration it is possible to arrange the experiment in such a way that each of the two beam splitters in its own reference frame analyzes a particle from an entangled pair before the other. Each particle then has to ''decide'' where to go before its twin particle makes its choice (even before the twin is forced to make a choice). Multisimultaneity predicts that in such a *before-before* configuration, the correlations disappear, in contrary to the quantum predictions.

Whereas quantum mechanics is nonlocal and independent of the time ordering, multisimultaneity assumes a nonlocal but time-ordered dependence between the events. Nevertheless, this alternative model is not in contradiction with any existing experimental data prior to the present experiment. Furthermore, it has the nice feature that it can be tested using existing technology. This means that before-before experiments are capable of acting as standard of time-ordered nonlocality (much as Bell experiments act as standard of locality).

Since it would have been very difficult to put conventional beam splitters in motion, we used traveling acoustic waves as beam splitters to realize a before-before configuration. It has been argued that the state of motion of the moving acoustic wave defines the rest frame of the beam splitters [11]. We would like to stress that a before-before experiment using detectors in motion has already been performed confirming quantum mechanics, i.e., the correlations did not disappear [34].

B. Experiment

As we have seen, an AOM is a realization of a moving beam splitter. We can then use our interferometers to perform a Bell experiment with moving beam splitters (Fig. 9) in order to confront quantum-mechanics predictions with multisimultaneity. We need to perform the experiment in the so-called before-before condition. The criterion given by special

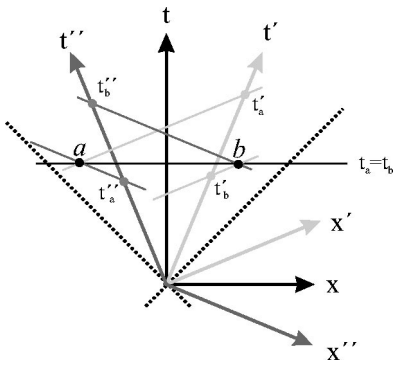

FIG. 10. The events a and b are simultaneous in reference frame x-t, whereas b is before a in a frame x'-t' moving at speed v in x-t, and a is before b in frame x''-t'', which is moving at speed $-v$ in x-t. The dashed lines represent the light cone.

relativity for the change in time ordering of two events in two reference frames counterpropagating at speed v (Fig. 10) reads

$$|\Delta t| < \frac{v}{c^2} d, \tag{31}$$

where Δt and d are, respectively, the time difference and distance between the two events in the laboratory frame [10]. This criterion is much more stringent than the spacelike separation condition $|\Delta t| < d/c$. Due to the high speed of the acoustic wave (2500 m/s), a distance of 55 m between the interferometers is enough, and allows us to realize the experiment inside our building. The permitted discrepancy on the time of arrival of the photons in the AOM is then, according to Eq. (31), $|\Delta t|_{max} = 1.53$ ps, corresponding to an optical path length of 0.46 mm in air.

We note that this distance is much smaller than the transit length of the photon across the acoustic wave (14.3 mm), and therefore the relevant points for the alignment are the points at which the choices exactly happen within the AOMs. According to multisimultaneity [11], as in Bohm's model (see the preceding section), one has to assume that the particles always follow a well defined trajectory in space time. In particular, the choices between transmission and reflection take place when the particles reach the edge of the diffraction lattice. This means in the case of AOMs that the choice of the outcome will only occur when the photon leaves the acoustic wave (independently of the transit length across). Hence the two events we have to consider for the alignment of the experiment are defined by the two points where the photons are leaving the AOMs for the second time, just before getting detected. We have to equalize the optical path length from the source to these points, with an error smaller than 0.46 mm.

1. Path-length alignment

The length difference between the fibers joining the source to the two interferometers can be measured with a precision of 0.1 mm using a low coherence interferometry method [21]. In each interferometer, the length of the light path from the output of the fiber to the second crossing of the AOM is measured manually with a precision of 0.5 mm. As this error is of the order of $|\Delta t|_{max}$, we scan the path-length difference by pulling on a 1-m-long fiber on Bob's side. One end of the fiber is fixed on a rail as the other one is fixed to a translation stage that is fixed to the rail. The fiber can be elongated over a range of about 10 mm in the elastic region. As the refractive index changes with the stress we need to calibrate the effective change in the optical path vs the fiber elongation (Fig. 11). We measure the visibility of the interference fringes for each step of 0.10 mm corresponding to a change of the path in air of 0.11 mm as given by the calibration. Since we measure 30 steps, the scanned length of 3 mm is much larger than the maximal error on the path-length difference measurement. This ensures that for some of the scanning steps we are in the before-before situation.

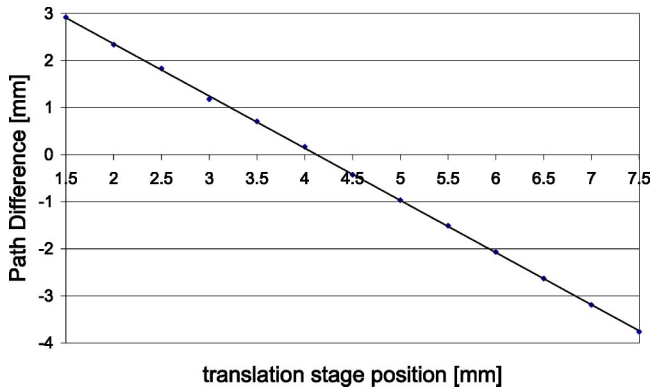

FIG. 11. Calibration of the optical path difference from the $\Delta t = 0$ situation vs the position of the translation stage.

2. Dispersion

A precise path alignment is not the only condition to observe the predicted disappearance of the correlations. The spreading of the wave packet due to the finite bandwidth of the photons combined with the chromatic dispersion of the optical fibers has to be smaller than Δt, too.

First, the coherence length of the single photons is determined by the filter after the source. With an 11-nm filter, the photons' coherence length is about 0.15 mm. Next, the chromatic dispersion spreads the photon wave packet. However, thanks to the energy correlation, the dispersion can be almost canceled. The requirement for the two-photon dispersion cancellation [35] is that the center frequency of the two-photon is equal to the zero dispersion frequency of the fibers. We measured this value on a 2-km fiber with a commercial apparatus (EG&G) which uses the phase-shift method. We found a value of 1313.2 nm for λ_0. We use 100 m of the same fiber assuming that the dispersion is constant along the fiber. We set the laser wavelength at half this value. Knowing the chromatic dispersion and conservatively assuming a 1-nm difference between the laser wavelength and $\lambda_0/2$, the pulse spreading over 100 m can be computed and is 0.2 ps (for more detail see Ref. [34]). This corresponds to a length of 0.06 mm in air, which is much smaller than the permitted discrepancy. The total spread is given by $\sqrt{0.15 + 0.06^2} = 0.152$ mm.

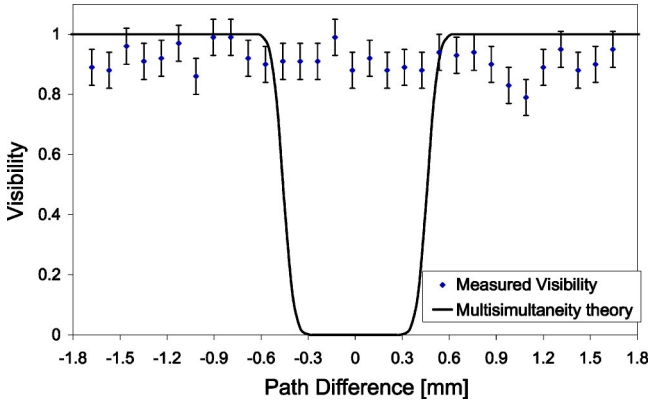

FIG. 12. Visibility vs path difference in the *before-before* situation. The dots are the measured visibilities vs path difference by step of 110 μm. The continuous line indicates the vanishing of the visibility as predicted by the multisimultaneity theory.

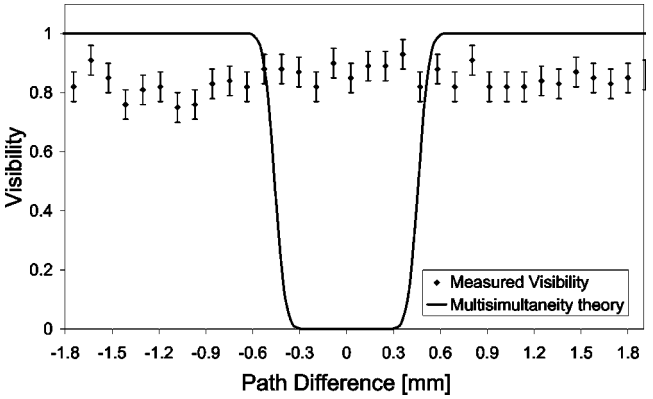

FIG. 13. Visibility vs path difference in the *after-after* situation.

3. Results

The theory predicts a disappearance of the correlations in the before-before case. The visibility depending on the path difference would be given by the function

$$V=\begin{cases}0 & \text{if } |x|<\Delta t\\ 1 & \text{otherwise.}\end{cases} \tag{32}$$

However, as the photons have a nonzero coherence length and are subject to spreading due to the dispersion, the correlations would vanish smoothly. For a path difference of x, the distribution of the times of arrival of the photons is given by

$$f(t)=\frac{1}{\sqrt{\pi}\sigma}\exp\left(-\frac{(t-x/c)^2}{2\sigma^2}\right). \tag{33}$$

Hence the visibility is given by the convolution of both functions:

$$V_{true}(x)=\int_{-\infty}^{+\infty}\frac{1}{\sqrt{\pi}\sigma}\exp\left(-\frac{(t-x/c)^2}{2\sigma^2}\right)V(t)dt. \tag{34}$$

In our case $\sigma=0.076$ mm due to dispersion and the photon coherence length. Figure 12 shows the measured visibility for different path difference and the expected curve according to multisimultaneity. It is clear that there is no disappearance of the correlations in the before-before situation.

Another intriguing situation is the opposite, where each measurement device is analyzing its photon in its own reference frame after the other analyzer photons. We call it after-after situation, for which multisimultaneity also makes predictions conflicting with quantum mechanics, and in our particular case disappearance of the correlations, as in the before-before situation [11,36].

Experimentally, the after-after situation is reached by inverting the direction of the acoustic waves, without changing the other adjustments of the experiment. Figure 13 shows a measurement of the visibility in function of the path difference. No change larger than the experimental fluctuations can be observed around the 0 difference point.

V. CONCLUSION

We have modified the usual two-photon Franson interferometry scheme by using AOMs instead of standard beam splitters. Adding a degree of freedom to the state of entangled photons leads to particular effects, such as two-photon beats. These are equivalent, for the two-photon interferences, to the usual one-photon beats. We have experimentally demonstrated two-photon interferences when the beat frequency is 0. In the other case when it is not null we have measured the beats.

As the reflection on an acoustic wave is equivalent to the reflection on a moving mirror, we have used our interferometers to test nonlocal correlations under different time orderings. In the before-before situation, each ''choice device'' is the first to analyze its photon in its own reference frame. In this situation the correlation would disappear if they were due to some time-ordered influence between the events, as multisimultaneity assumes. Experimentally, we do not see any vanishing of the correlations. Hence, not only, the quantum correlations cannot be explained by local common causes as demonstrated by violating Bell inequality, but moreover one cannot maintain any causal explanation in which an earlier event influences a later one by arbitrarily fast communication.

In conclusion, correlations reveal somehow dependence between the events. But regarding quantum correlations, our experiment shows that this dependence does not correspond to any real time ordering.

ACKNOWLEDGMENTS

This work would not have been possible without the financial support of the ''Fondation Odier de Psychophysique'' and the Swiss National Science Foundation. We thank Valerio Scarani and Wolfgang Tittel for very stimulating discussions and François Cochet of Alcatel Cable Suisse SA for having placed at our disposal the chromatic dispersion measurement instrument.

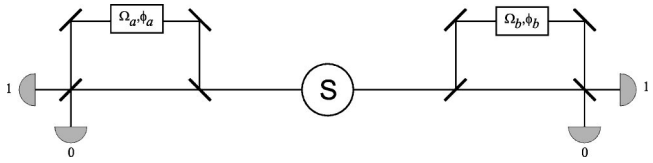

FIG. 14. Quantum key distribution scheme with the entangled photon pair. Depending on the phases and frequency shifts, correlations can appear between the detector outputs. If $\Omega_a+\Omega_b=0$, key distribution can be achieved by changing the phases ϕ_a and ϕ_b, as if $\phi_a+\phi_b=0$ the frequencies Ω_a and Ω_b have to be changed.

APPENDIX: FREQUENCY SHIFT TWO-PHOTON QUANTUM CRYPTOGRAPHY

The quantum theory has allowed the development of new cryptographic protocols, in particular, quantum key distribution. Two people, Alice and Bob, can create a shared secret key by exchanging quantum particles. Coding bits into photons whose states are randomly chosen between nonorthogonal bases prevents any effective attack by a third person. A similar protocol based on the quantum correlations between entangled particles has been proposed [37]. In this appendix, we present two schemes for quantum cryptography using two-photon correlations. The first one uses the phenomenon of beats as described in Sec. II, to simulate two bases at 45°. The second is the analogue with two photons to the interferometric scheme with frequency separation [15].

1. Cryptography with pseudocomplementary basis

First, we briefly review the principle of the two-photon quantum cryptography with phase coding [14,37,38]. It is based on Franson two-photon interferences (Fig. 14). Alice and Bob chose a phase in their respective interferometers (corresponding to the choice of a basis). When the bases are compatible ($\phi_1+\phi_2=0$) there is a perfect correlation between the outputs of both interferometers, the correlation coefficient E is equal to 1. When the bases are incompatible ($\phi_1+\phi_2=\pm\pi/2$) the correlation coefficient vanishes, the outcomes are completely independent and random. This is summarized in the following table.

Alice ϕ_1	Bob ϕ_2	$\phi_1+\phi_2$	E
0	0	0	1
0	$-\pi/2$	$-\pi/2$	0
$\pi/2$	0	$\pi/2$	0
$\pi/2$	$-\pi/2$	0	1

Those correlations can be used to create a secret key between Alice and Bob. This scheme could be implemented with our setup if Alice and Bob set their frequency shifts such that $\Omega^0=0$. They can change their respective phases by modulating the phase in one arm (i.e., by changing the length). However, they can also change the phases by changing the phase of the synchronization signal on each side as we have seen in Sec. III E.

Instead of changing the phase, Alice and Bob can change the frequency of the photons. As they are looking for interferences between the short-short and long-long paths, beats will appear if the sum of the frequency shift is not zero (Sec. III F). The probability coincidences are given by Eq. (4) where the global phase is fixed to 0.

$$p_{++}=p_{++}=\frac{1+\cos[\phi_1+\phi_2+(\Omega_1+\Omega_2)t]}{4}, \quad \text{(A1)}$$

$$p_{+-}=p_{-+}=\frac{1-\cos[\phi_1+\phi_2+(\Omega_1+\Omega_2)t]}{4}. \quad \text{(A2)}$$

Putting $\Omega_1+\Omega_2=0$ we find the previous table. But we could change $\Omega_1+\Omega_2=\Omega^0$ without changing $\phi_1+\phi_2$. Hence if we set $\phi_1+\phi_2=0$ we have

$$p_{++}=p_{--}=\frac{1+\cos(\Omega t)}{4}, \quad \text{(A3)}$$

$$p_{+-}=p_{-+}=\frac{1-\cos(\Omega t)}{4}. \quad \text{(A4)}$$

If $\Omega^0=0$ we find the perfectly correlated case, otherwise there will be an additional phase of $\Omega^0 t$ which is not equal to $\pm\pi/2$, as in the phase coding. However, as the emission time of the photons is not known, the $\Omega^0 t$ value is uniformly distributed, so the mean value of $\cos(\Omega^0 t)$ averaged over time is equal to 0, corresponding to the noncorrelated case. We can then write a similar table as the previous one but with the phases ϕ_i replaced by the frequency shifts Ω_i:

Alice Ω_1	Bob Ω_2	$\Omega_1+\Omega_2$	$\langle E\rangle$
0	0	0	1
0	$-\Omega$	$-\Omega$	0
Ω	0	Ω	0
Ω	$-\Omega$	0	1

We should keep in mind that the correlation value in this table is only a mean value, therefore we call it a pseudocomplementary basis. If Eve knows the detection time of a photon she could follow the beats; she will always know the value of $\cos(\Omega^0 t)$ and can wait for a time $t_{Eve}=2\pi n/\Omega^0$, such that $p_{++}=p_{--}=1/2$, so as to know which detector clicked on Alice's side. Therefore the detection time should be kept secret as long as the photon did not reach Bob's side. However, Alice and Bob have to perform a coincidence detection to select only the short-short and long-long events. In order to discriminate these events, the time uncertainty δt on the coincidence has to be smaller than the time difference $\Delta l/c$ between short and long arms. Moreover, if the uncertainty on the detection time sent by Alice is greater than the beats period, Eve cannot extract any information on the timing. This requires $1/2\pi\Omega^0<\delta t$. For example, if $\Omega^0=400$ MHz we have $\delta t>0.4$ ns, so that $\Delta l/c$ should be greater than 0.4 ns, which is the case in our experiment ($\Delta l/c\simeq 1.5$ ns).

Finally, if we imagine that Eve is able to measure when the photon passes (by quantum nondemolition measure-

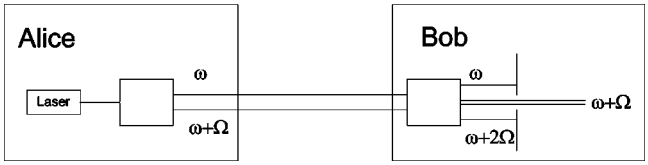

FIG. 15. Schematic of a quantum cryptography scheme using single-photon phase modulation.

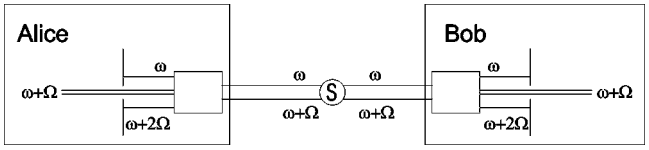

FIG. 16. Schematic of a quantum cryptography scheme using two-photon phase modulation.

ment), she can again follow the beats and set her measurement time such that she is in perfect correlation with Alice. To avoid this attack, Alice should choose randomly when she sends the photon to Bob. Again, the uncertainty on the emission time δt has to be greater than $1/2\pi\Omega^0$.

Such a scheme of quantum key distribution would not be easy to implement because it requires stabilization of the interferometers as for the phase coding. Moreover, fast changes of the frequencies of the AOMs are needed.

2. Two-photon quantum cryptography with phase modulation

In contrary to the preceding scheme, where one-photon interferences occur between two spatially separated paths, a scheme where the paths are frequency separated has been proposed and realized in Refs. [15,39]. The experimental setup was done using faint laser pulses, which, for this purpose, is equivalent to a single-photon scheme. It has the advantage of not requiring an interferometer's stabilization. We will see that this one-photon scheme can be generalized to a two-photon one. But first, we briefly review the original scheme. Alice creates a photon in a superposition of two states of different frequencies by modulating light at frequency Ω (Fig. 15) and by applying a phase difference φ_a.

Hence the state of a photon at frequency ω becomes

$$|\omega\rangle \rightarrow |\omega\rangle + e^{i\varphi_a}|\omega+\Omega\rangle. \tag{A5}$$

Bob analyzes the photon by applying a similar operation with a phase φ_b,

$$|\omega\rangle + e^{i\varphi_a}|\omega+\Omega\rangle \rightarrow |\omega\rangle + e^{i\varphi_a}|\omega+\Omega\rangle + e^{i\varphi_b}|\omega+\Omega\rangle + e^{i(\varphi_a+\varphi_a)}|\omega+2\Omega\rangle, \tag{A6}$$

and selecting only the $\omega+\Omega$ frequency. The remaining state is

$$(e^{i\varphi_a}+e^{i\varphi_b})|\omega+\Omega\rangle \sim (1+e^{i(\varphi_a-\varphi_b)})|\omega+\Omega\rangle. \tag{A7}$$

Such a state can be used to implement quantum key distribution with the B92 protocol [40].

The generalization to two-photon interferometry can be done because each single-photon cryptographic scheme (Fig. 16) is equivalent to a two-photon scheme up to local unitary transformation [14]. In this case, the equivalent scheme (Fig. 16) consists in a source-emitting a state

$$|\omega+\Omega\rangle|\omega+\Omega\rangle + |\omega\rangle|\omega\rangle. \tag{A8}$$

When Alice and Bob apply the transformation given by Eq. (A5) on their side, the state becomes

$$|\omega+\Omega\rangle|\omega+\Omega\rangle + |\omega\rangle|\omega\rangle \rightarrow |\omega+\Omega\rangle|\omega+\Omega\rangle + e^{i\varphi_a}|\omega+2\Omega\rangle|\omega+\Omega\rangle + e^{i\varphi_b}|\omega+\Omega\rangle|\omega+2\Omega\rangle + e^{i(\varphi_a+\varphi_b)}|\omega+2\Omega\rangle|\omega+2\Omega\rangle + |\omega\rangle|\omega\rangle + e^{i\varphi_a}|\omega+\Omega\rangle|\omega\rangle + e^{i\varphi_b}|\omega\rangle|\omega+\Omega\rangle + e^{i(\varphi_a+\varphi_b)}|\omega+\Omega\rangle|\omega+\Omega\rangle. \tag{A9}$$

In order to create the state of Eq. (A8) by down-conversion, the laser pump has to be in the state

$$|\omega_p\rangle + |\omega_p+\Omega/2\rangle. \tag{A10}$$

It will generate the state

$$\int |\omega+\Omega+\delta\omega\rangle|\omega+\Omega-\delta\omega\rangle + |\omega_p+\delta\omega\rangle|\omega_p-\delta\omega\rangle, \tag{A11}$$

which does not need to be filtered right after the pump, as the photons with an energy other than ω will not contribute to the key exchange (they will be filtered on each side).

After the filters, the following state remains:

$$(1+e^{i(\varphi_a+\varphi_b)})|\omega+\Omega\rangle|\omega+\Omega\rangle. \tag{A12}$$

This state can be used to implement the two-photon quantum key distribution. Moreover, this scheme has only one output. It can be generalized to a system with two outputs (BB84) by doing the following frequency transformation:

$$|\omega\rangle \rightarrow |\omega\rangle + e^{i\varphi_a}|\omega+\Omega\rangle + e^{-i\varphi_a}|\omega-\Omega\rangle. \tag{A13}$$

[1] P.G. Kwiat *et al.*, Phys. Rev. Lett. **75**, 4337 (1995).
[2] J.D. Franson, Phys. Rev. Lett. **62**, 2205 (1989).
[3] J. Brendel, E. Mohler, and W. Martienssen, Europhys. Lett. **20**, 575 (1992).
[4] W. Tittel, J. Brendel, H. Zbinden, and N. Gisin, Phys. Rev. Lett. **81**, 3563 (1998).
[5] J. Brendel, N. Gisin, W. Tittel, and H. Zbinden, Phys. Rev. Lett. **82**, 2594 (1999).
[6] R.T. Thew, S. Tanzilli, W. Tittel, H. Zbinden, and N. Gisin, Phys. Rev. A **66**, 062304 (2002).
[7] W. Tittel and G. Weihs, Quantum Inf. Comput. **1**, 2 (2001).
[8] A. Stefanov, H. Zbinden, A. Suarez, and N. Gisin, Phys. Rev. Lett. **88**, 120404 (2002).
[9] T. Maudlin, *Quantum Non-Locality and Relativity*, 2nd ed. (Blackwell, Oxford, 2002).
[10] A. Suarez and V. Scarani, Phys. Lett. A **232**, 9 (1997).
[11] A. Suarez, Phys. Lett. A **269**, 293 (2000).
[12] *Fiber Optic Test and Measurement*, edited by D. Derickson (Prentice-Hall, Englewood Cliffs, NJ, 1998).
[13] Z.Y. Ou and L. Mandel, Phys. Rev. Lett. **61**, 50 (1988).
[14] N. Gisin, G. Ribordy, W. Tittel, and H. Zbinden, Rev. Mod. Phys. **74**, 145 (2002).
[15] J.-M. Merolla, Y. Mazurenko, J.-P. Goedgebuer, L. Duraffourg, H. Porte, and W.T. Rhodes, Phys. Rev. A **60**, 1899 (1999).
[16] P.C. Sun, Y. Mazurenko, and Y. Fainman, Opt. Lett. **20**, 1062 (1995).
[17] R.P. Feynman, *Lectures on Physics* (Addison-Wesley, Reading, MA, 1969), Vol. 3.
[18] D.M. Greenberger, M.A. Horne, and A. Zeilinger, Phys. Today **46**, 22 (1991).
[19] P.D.D. Schwindt, P.G. Kwiat, and B.G. Englert, Phys. Rev. A **60**, 4285 (1999).
[20] G. Jaeger, A. Shimony, and L. Vaidman, Phys. Rev. A **51**, 54 (1995).
[21] W. Tittel, J. Brendel, B. Gisin, T. Herzog, H. Zbinden, and N. Gisin, Phys. Rev. A **57**, 3229 (1998).
[22] S. Tanzilli, H. De Riedmatten, W. Tittel, H. Zbinden, P. Baldi, M. De Micheli, D.B. Ostrowsky, and N. Gisin, Electron. Lett. **37**, 26 (2001).
[23] S. Tanzilli, W. Tittel, H. De Riedmatten, H. Zbinden, P. Baldi, M. De Micheli, D.B. Ostrowsky, and N. Gisin, EPJdirect **18**, 155 (2002).
[24] B.E.A. Saleh and M.C. Teich, *Fundamentals of Photonics* (Wiley, New York, 1991).
[25] A. Yariv, *Quantum Electronics*, 3rd ed. (Wiley, New York, 1989).
[26] J. Billigham and A.C. King, *Wave Motion* (Cambridge University Press, Cambridge, 2000).
[27] *Handbook of Optics*, 2nd ed. (McGraw-Hill, New York, 1995), Vol. 2, p. 33.51.
[28] A. Aspect, J. Dalibard, and G. Roger, Phys. Rev. Lett. **49**, 1804 (1982); G. Weihs, T. Jennewein, C. Simon, H. Weinfurter, and A. Zeilinger, *ibid.* **81**, 5039 (1998); M.A. Rowe, D. Kielpinski, V. Meyer, C.A. Sackett, W.M. Itano, C. Monroe, and D.J. Wineland, Nature (London) **409**, 791 (2001).
[29] J.S. Bell, Physics (Long Island City, N.Y.) **1**, 195 (1964); *Speakable and Unspeakable in Quantum Mechanics* (Cambridge University Press, Cambridge, 1987).
[30] D. Bohm, Phys. Rev. **85**, 166 (1952); D. Bohm and B.J. Hilley, *The Undivided Universe* (Routledge, New York, 1993).
[31] Ph.H. Eberhard, Nuovo Cimento Soc. Ital. Fis., B **38B**, 75 (1977); **46**, 392 (1978); G.C. Ghirardi, A. Rimini, and T. Weber, Lett. Nuovo Cimento Soc. Ital. Fis. **27**, 293 (1980).
[32] Ph.H. Eberhard, in *Quantum Theory and Pictures of Reality*, edited by W. Schommers (Springer, New York, 1989), pp. 169–215.
[33] N. Bohr, Phys. Rev. **48**, 696 (1935).
[34] H. Zbinden, J. Brendel, N. Gisin, and W. Tittel, Phys. Rev. A **63**, 022111 (2001); N. Gisin, V. Scarani, W. Tittel, and H. Zbinden, Ann. Phys. (Leipzig) **9**, 831 (2000).
[35] A.M. Steinberg, P.G. Kwiat, and R.Y. Chiao, Phys. Rev. Lett. **68**, 2421 (1992); T.S. Larchuk, M.C. Teich, and B.E.A. Saleh, Phys. Rev. A **52**, 4145 (1995).
[36] A. Suarez, Phys. Lett. A **236**, 383 (1997).
[37] A.K. Ekert, Phys. Rev. Lett. **67**, 661 (1991).
[38] G. Ribordy, J. Brendel, J.-D. Gauthier, N. Gisin, and H. Zbinden, Phys. Rev. A **63**, 012309 (2000).
[39] L. Duraffourg, J.-M. Merolla, J.-P. Goedgebuer, Y. Mazurenko, and W.T. Rhodes, Opt. Lett. **26**, 1427 (2001).
[40] C.H. Bennett, Phys. Rev. Lett. **68**, 3121 (1992).